Pré-Publicações do Departamento de Matemática
Universidade de Coimbra
Preprint Number 14–23

MOLECULAR TRANSPORT IN VISCOELASTIC MATERIALS: MECHANISTIC PROPERTIES AND CHEMICAL AFFINITIES

J.A. FERREIRA, P. DE OLIVEIRA, P.M. DA SILVA AND LAURENT SIMON

Abstract: Simulations show that the kinetics of permeant fluids in viscoelastic matrices depends on the rheological and chemical properties of the material. Fick's law fails to describe transport through viscoelastic materials because of the stress exerted on the incoming fluid which causes a delay. Reversible binding to immobilizing sites also retard permeation of molecules. The effects of mechanical properties and chemical affinities of materials on the transport of solutes are studied. An integro-partial-differential equation (IPDE) is used to model the transport. While the differential part of the equation is represented by an elliptic operator, the integral part, describes the contributions of stress and reversible binding. The stability of the model is investigated. The steady-state flux and effective time constant are calculated. The lag time is also studied using multiple integration. Subsequent analyses reveal the dependence of the steady-state flux, the effective time constant, the lag time on the Young modulus, the viscosity and the binding/unbinding rates. The results presented in this paper make it possible to tune the mechanical and chemical properties to achieve a desired transport profile.
Keywords: partial integro-differential equation, viscoelasticity, Laplace transform

1. Introduction

Viscoelastic materials continue to play a pivotal role in applications, such as controlled release systems, chemical protective clothing and impermeable liners. In controlled release systems, these materials are used as carriers ([14]) and coatings designed to mask the taste of a medication ([16]). Delivery via the oral route is difficult for proteins produced in bioreactors because of enzymes present in the gastrointestinal tract. In addition, the short life of these molecules makes it necessary to administer several injections to maintain a therapeutic plasma concentration. The ideal situation would be to shield the drug until it reaches the target site, at which point the carrier is able to unload its cargo in a predetermined manner. Protective clothing is important to guard against chemical hazards or biohazards. Some of these compounds are absorbed through chemical protective clothing permeation, the skin barrier and the viable epidermis, followed by distribution into the blood capillaries

Received June 25, 2014.

resulting in systemic poisoning. Nanotechnology-based materials are investigated for providing protection in these cases ([24]). Contrary to controlled release technologies, efforts are devoted to developing a strong barrier to prevent the absorption of chemicals. Impermeable liners, such as geomembranes, are designed to reduce risks associated with the diffusion of pollutants in the environment ([13]). To serve as effective sealants against contaminants, the mechanical properties of the membrane have to be well understood. Studies should also shed light on how chemicals are being transported through these polymeric sheets ([13]) to prevent seepage of pollutants.

In spite of the notable success and progress, the lack of adequate mathematical models that account for the permeant/polymer structures limits further development in key research areas. A measure of the time it takes to achieve a steady-state condition (effective time) and the first moment when a concentration of permeant is detected (lag time) is sometimes missing from the literature or not written as an explicit function of the system characteristics. A clear understanding of the links between the performance criteria and these key features would provide experimentalists with a great insight into the governing transport mechanisms.

The motion of a fluid through a polymeric matrix depends not only on the properties of the fluid but also on the mechanistic and chemical properties of the material. As a response to the strain caused by permeation, the matrix offers a resistance in the form of a stress exerted on the incoming fluid. This means that the brownian motion, underlying Fickian diffusion, is delayed by the viscoelasticity of the matrix. Furthermore, if the material is reactive, as it is the case of reversible binding to immobilizing sites, the transport of the solvent is further delayed.

Transport through viscoelastic matrices and reactive matrices has received considerable attention by both experimentalists and theorists. In [18] and [19], the transport of a fluid through a reactive matrix is studied but no viscoelastic effects are considered. Recheares address a simplified mechanical model in [8] and [9] and establish an expression for the effective time. In these papers, the mechanical properties of the matrix is described by a Maxwell or a Maxwell-Voigt model ([1]) and lag time is not computed.

In the present paper, a generalized Maxwell model is used to examine viscoelastic effects. Furthermore, the chemical interaction between the permeant and the matrix, that is the binding to immobilizing sites in the matrix, which is a feature common to many applications, is also added to the

model. The problem can be modeled by an integro-partial-differential equation (IPDE), where the differential part represents the Fickian diffusion. The integral operators in the equation include memory terms that describe the viscoelastic behavior and the chemical properties of the material. The stability of the IPDE, relative to perturbations of the initially conditions, can be proved by a technique presented in [25]. The theoretical restrictions needed to establish stability have a sound physical meaning and are used to select meaningful parameters in the computations. This model allows researchers to use experimental rheological information about elasticity and viscosity of the material. Data generated by experimentalists are easily incorporated in the model. As Maxwell generalized model may include as many parameters as needed, stress-strain profiles from laboratory data can be described accurately.

We implement an analytical approach in order to develop closed formulas for the steady fluxes, and the time constants. These formulas are derived without explicit knowledge of the solution and highlight the dependence of the solution on the phenomenological parameters of the model. The theory of Laplace transforms is employed to characterize the steady-state flux and the effective time constant that can be interpreted statistically as the waiting time to achieve equilibrium in the system. An expression for the concept of lag time is provided using multiple integration in space and time. The dependence of the steady-state flux, the effective time constant and the lag time on the mechanical and chemical parameters of the model is fully analyzed. These findings are important tools for designing a system that behaves in a predefined manner.

Section 2 of this contribution focuses on an integro-differential model of transport through a viscoelastic matrix. The stability of the model is analysed. The effective time constant and lag time are computed. In Section 3, the joint influence of viscoelasticity and reversible binding is discussed. Numerical simulations in Sections 2 and 3 are performed with an Implicit-Explicit finite difference method. Conclusions are drawn in Section 4.

2. Diffusion and viscoelastic properties

2.1. Mathematical model. We consider a fluid diffusing through a viscoelastic cylindrical matrix $\Omega \subset \mathbb{R}^3$ with a boundary defined by $\partial\Omega = \Gamma_{in} \cup \Gamma_{out} \cup \Gamma_L$, where Γ_L is insulated. The matrix is initially void of the fluid, which later enters the material at Γ_{in}, diffuses through the system and

reaches Γ_{out} where it is immediately removed (Fig. 1). The incoming fluid

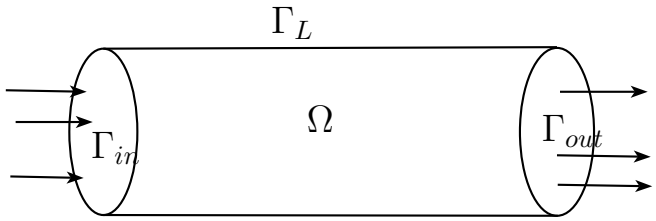

FIGURE 1. Geometry of the viscoelastic cylindrical matrix.

strains the molecular chains of the matrix which respond by exerting a stress in the opposite direction.

Viscoelasticity is described by analogical models where the elastic properties are represented by springs and the viscous properties by dashpots ([1]). A spring and a dashpot can be arranged in parallel (Kelvin model) or in series (Maxwell model) to reproduce a certain viscoelastic behaviour. However, single Kelvin and Maxwell elements are of limited use when describing an experimental stress-strain relation. In fact, in both models, only two free parameters are available (the Young's modulus of the spring and the viscosity of the dashpot) to fit an experimental plot. A number n of Maxwell (Kelvin) elements can be associated in parallel (series) to obtain a model with $2n$ free parameters which lead to an accurate fit of experimental results. In this paper, we define the relationship between the stress σ and the strain ϵ using a Maxwell generalized model with n Maxwell arms and an isolated spring (Figure 2).

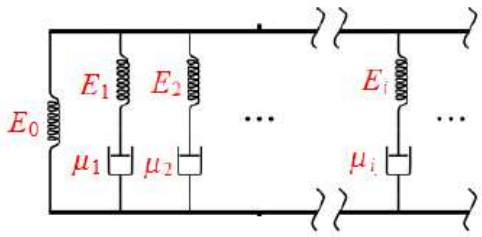

FIGURE 2. Maxwell generalyzed model representation.

The stress response of Maxwell arm i is obtained as the solution of the linear differential equation,

$$\frac{E_i}{\mu_i}\sigma_i + \frac{\partial \sigma_i}{\partial t} = E_i \frac{\partial \epsilon}{\partial t},\ i = 1, ..., n, \tag{1}$$

where E_i stands for the Young's modulus of arm i and μ_i its viscosity. The isolated spring with the Young's modulus E_0 has an elastic behaviour and consequently $\sigma_0 = E_0\epsilon$, where σ_0 represents its stress response to the strain ϵ. The total stress results from the sum of σ_i, $i = 0, 1, ..., n$, and, assuming that $\sigma_i(0) = 0$, it can be given the form

$$\sigma = \int_0^t (E_{0+} \sum_{i=1}^{n} E_i e^{-\frac{t-s}{\tau_i}}) \frac{\partial \epsilon}{\partial s} ds \text{ in } \Omega \times \mathbb{R}^+, \tag{2}$$

where $\tau_i = \frac{\mu_i}{E_i}$ is the relaxation time of arm i. The parameter σ represents in fact the absolute value of the stress. However, when the meaning of σ, as a barrier to the permeation, is to be considered, Eq. (2) must reflect the opposite signs of σ and ϵ.

If u represents the concentration of the incoming fluid in Ω, we assume that $\epsilon = \alpha u$, where α is a dimensional constant. The ansatz appears physically sound and it has been adopted by several authors ([4], [5], [17], [26]). As $\frac{\partial u}{\partial t} > 0$, the polymer exerts on the fluid a force

$$\sigma = -\alpha \int_0^t (E_{0+} \sum_{1}^{n} E_i e^{-\frac{t-s}{\tau_i}}) \frac{\partial u}{\partial s} ds \text{ in } \Omega \times \mathbb{R}^+. \tag{3}$$

The assumption $\frac{\partial u}{\partial t} > 0$ is phenomenological and is a consequence of the fact that the matrix is initially void and continuously fed by the fluid.

If $E_0 = 0$, Eq. (3) represents a material that completely relaxes as $\sigma(t) \to 0$ when $t \to \infty$. Otherwise, there is no complete relaxation which means a permanent bonding exists between the molecular chains.

The diffusion of the fluid in Ω is described by

$$\frac{\partial u}{\partial t} = \nabla.(D\nabla u) + \nabla.(D_v \nabla \sigma) \text{ in } \Omega \times \mathbb{R}^+, \tag{4}$$

where σ is defined in Eq (3); D and D_v correspond to the diffusion and stress-driven diffusion matrices, respectively. The units used in Eqs (3) and (4) are presented in Annex I.

For $n = 1$, Eqs (3) and (4) lead to the models in [8], [9], [17] and [26]. As shown in [6] and [7], the constant D_v is positive and has a precise physical meaning whereas the stress is of opposite sign to the strain. The authors in [17] and [26] applied an equation of type (4) but use the Kelvin-Voigt model to describe the relation ship between the stress and the strain. These last two contributions essentially present numerical simulations. In addition, the time constant was not determined.

Replacing the stress σ in Eq. (4) and assuming that the matrix is initially void of the fluid, we obtain the following equation

$$\frac{\partial u}{\partial t} = \nabla \cdot (D - \widetilde{D_v}\widehat{E})\nabla u + \int_0^t k(t-s)\nabla \cdot (\widetilde{D_v}\nabla u(s))ds, \tag{5}$$

where $\widetilde{D_v} = \alpha D_v$, $\widehat{E} = \sum_{i=0}^{n} E_i$ and

$$k(s) = \sum_{i=1}^{n} \frac{E_i}{\tau_i} e^{-s/\tau_i} \tag{6}$$

In what follows, we drop the tilde in D_v. Equation (5) can assume the conservative form

$$\frac{\partial u}{\partial t} = -\nabla . J, \tag{7}$$

with the flux J defined by

$$J(x,t) = -(D - D_v\widehat{E})\nabla u - D_v \int_0^t k(t-s)\nabla u(s)ds. \tag{8}$$

The model is completed with the following boundary and initial conditions

$$\begin{cases} u = u_0 \text{ on } \Gamma_{in} \times \mathbb{R}^+, \\ u = 0 \text{ on } \Gamma_{out} \times \mathbb{R}^+, \\ J = 0 \text{ on } \Gamma_L \times \mathbb{R}^+, \end{cases} \tag{9}$$

and

$$\{ \ u(x,0) = 0, \ x \in \Omega. \tag{10}$$

The boundary condition on Γ_{out} means that the fluid is immediately removed. Condition $J = 0$ implies that the boundary Γ_L is insulated. As a result if we extend Eq. (7) to the boundary Γ_{out} we obtain $\sigma = 0$ at Γ_{out}. Other conditions on u, such as a Robin condition of type $u(x,t) = k_p u_{ext}$,

can be considered. This formulation includes the permeability constant k_p and the exterior fluid concentration u_{ext}. Our results can be generalized to this case but the approach would involve more complex computations. We assume that $D - D_v\widehat{E}$ is a diagonal matrix. As the entries represent the overall Fickian diffusion, the matrix needs to be positive definite. We will study if this condition is sufficient to prove stability.

In what follows, we assume that

$$0 < D_{min} < D_{ii},\ 0 < D_{v,ii} < D_{v,max},\ \ i = 1, 2, 3$$

where D_{ii} and $D_{v,ii}$ stand for the diagonal entries of D and D_v, respectively. If $D_{min} - \widehat{E}D_{v,max} > 0$, then the bilinear form

$$a(u, v) = ((D - \widehat{E}D_v)\nabla u, \nabla v),\ u,\ v \in H^1_\Gamma(\Omega),$$

where $H^1_\Gamma(\Omega) = \{v \in H^1(\Omega) : v = 0\ on\ \Gamma_{on} \cup \Gamma_{out}\}$, is elliptic in $[H^1_\Gamma(\Omega)]^2$ and problem (5) has a unique solution ([10], [11]). The stability analysis follows the method outline in [25].

Let $u_\gamma(x, t) = e^{\gamma t}u(x, t)$. It can be shown that u_γ is solution of

$$\begin{cases} \dfrac{\partial u_\gamma}{\partial t} - \gamma u_\gamma = \nabla.((D - \widehat{E}Dv)\nabla u_\gamma) \\ \qquad\qquad + \displaystyle\int_0^t k_\gamma(t-s)e^{\gamma(t-s)}\nabla.(D_v\nabla u_\gamma(s))ds,\ \text{in } \Omega,\ t > 0, \\ u_\gamma(x, 0) = w_0(x),\ x \in \Omega, u_\gamma(x, t) = 0,\ x \in \partial\Omega,\ t > 0, \end{cases} \tag{11}$$

where $k_\gamma(s) = e^{\gamma s}k(s)$. The energy method leads to

$$\begin{aligned} &\frac{1}{2}\frac{d}{dt}\|u_\gamma(t)\|^2 - \gamma\|u_\gamma(t)\|^2 \\ &\qquad = -\|\sqrt{D - \widehat{E}Dv}\nabla u_\gamma(t)\|^2 - \int_0^t k_\gamma(t-s)\,(D_v\nabla u_\gamma(s), \nabla u_\gamma(t))\,ds, \end{aligned} \tag{12}$$

where $\|.\|$ denotes both the norm of $L^2(\Omega)$ and $[L^2(\Omega)]^3$. The symbol $(.,.)$ is used to describe the inner products of these spaces. The notation $\sqrt{A}$ represents a matrix whose entries are the roots of the entries of A.

Assuming that $\gamma \leq \min_i \frac{1}{\tau_i}$, then

$$\int_0^t k_\gamma(t-s)ds \leq \beta_\gamma = \sum_{i=1}^{n} \frac{E_i}{1 - \gamma\tau_i}.$$

As

$$\int_0^t k_\gamma(t-s)\|\nabla u_\gamma(s)\|ds\cdot\|\nabla u_\gamma(t)\| \leq \frac{1}{2}\int_0^t k_\gamma(t-s)\|\nabla u_\gamma(s)\|^2 ds + \frac{\beta_\gamma}{2}\|\nabla u_\gamma(t)\|^2, \tag{13}$$

we obtain

$$\frac{1}{2}\frac{d}{dt}\|u_\gamma(t)\|^2 + 2\left(D_{min} - \widehat{E}D_{v,max} - \gamma C_p - \frac{1}{2}D_{v,max}\beta_\gamma\right)\|\nabla u_\gamma(t)\|^2 \leq D_{v,max}\int_0^t k_\gamma(t-s)\|\nabla u_\gamma(s)\|^2 ds,\ t>0. \tag{14}$$

In (14) C_p is such that $\|v\|^2 \leq C_p\|\nabla v\|^2$, $\forall v \in H^1_\Gamma(\Omega)$. Equation (14) leads to

$$\|u_\gamma(t)\|^2 + 2\left(D_{min} - D_{v,max}(\widehat{E} - \frac{\beta_\gamma}{2}) - \gamma C_p\right)\int_0^t \|\nabla u_\gamma(s)\|^2 ds \leq \|u_0\|^2 + D_{v,max}\int_0^t\int_0^\eta k_\gamma(\eta-s)d\eta\|\nabla u_\gamma(s)\|^2 ds d\eta,\ t\geq 0. \tag{15}$$

From (15) we have

$$\|u_\gamma(t)\|^2 + 2\left(D_{min} - D_{v,max}(\widehat{E}+\beta_\gamma) - \gamma C_p\right)\int_0^t \|\nabla u_\gamma(s)\|^2 ds \leq \|u(0)\|^2,\ t\geq 0. \tag{16}$$

If

$$D_{min} - D_{v,max}(\widehat{E} + \sum_{i=1}^n E_i) > 0, \tag{17}$$

then there exists $\gamma > 0$ such that

$$\|u(t)\|^2 + 2\left(D_{min} - D_{v,max}(\widehat{E}+\beta_\gamma) - \gamma C_p\right)\int_0^t e^{-2\gamma(t-s)}\|\nabla u(s)\|^2 ds \leq e^{-2\gamma t}\|u(0)\|^2,\ t\geq 0, \tag{18}$$

which proves that the model is stable.

Note that Eq. (17) is a stronger condition than simply requiring that the diagonal matrix $D - D_v\widehat{E}$ be positive definite. For the rest of this work, we assume that condition (17) holds.

2.2. Identification of Dynamic Characteristics. The fluid flow properties are the same over any cross section of Ω perpendicular to the cylinder axis. This means that the permeation of the fluid can be represented by a one dimensional equation in space, with Dirichlet boundary conditions.

Closed-form expressions for lag time (t_{lag}) and the effective time constant (t_{eff}) are derived in this section. The performance of these metrics has been investigated by several researchers ([2], [8], [15], [19], [20], [21], [23]). Simulations are conducted to study how accurately they predict the steady-state flux.

2.2.1. *Lag time.* The first appearance of a penetrant at Γ_{out} occurs at the first instant t^* such that $Q(t^*) \neq 0$, where $Q(t)$ is the total mass released. The time constant lag time is an approximation of t^* and monitors the moment when a detectable concentration is measured in a receiver cell, at Γ_{out}, as is defined in what follows. From a mathematical point of view, an asymptote to the graph of Q is computed and t_{lag} is its intersection with the t axis.

Definition 2.1. *The lag time is defined by*

$$t_{lag} = -\frac{b}{m},$$

where $m = \lim_{t\to\infty} \dfrac{Q(t)}{t}$ *and* $b = \lim_{t\to\infty} \left(Q(t) - \lim_{s\to\infty} \dfrac{Q(s)}{s} t \right)$.

According to a method first introduced by Frisch in [12] and further studied in [3], Eq. (4) is integrated twice in space and once in time, resulting in

$$\int_0^L \int_x^L u(y,t)dydx = -LQ(t) + \int_0^t \int_0^L J(x,s)dxds, \tag{19}$$

where $\Omega = [0, L]$, $Q(t) = \displaystyle\int_0^t J(L,s)ds$ and J is the flux defined in (8). From Eqs. (8) and (19) we have

$$\begin{aligned} \int_0^L \int_x^L u(y,t)dydx = -LQ(t) - \int_0^t \int_0^L D^* \frac{\partial u}{\partial x}(x,s)dxds \\ -D_v \int_0^t \int_0^L \int_0^s \sum_{i=1}^n \frac{E_i}{\tau_i} e^{-\frac{s-\tau}{\tau_i}} \frac{\partial u}{\partial x}(x,\tau)d\tau dxds, \end{aligned} \tag{20}$$

where $D^* = D - D_v\widehat{E}$.

As

$$-\int_0^t\int_0^L D^*\frac{\partial u}{\partial x}(x,s)dxds = D^*u_0t \tag{21}$$

and

$$\int_0^t\int_0^L\int_0^s\sum_{i=1}^n\frac{E_i}{\tau_i}e^{-\frac{s-\tau}{\tau_i}}\frac{\partial u}{\partial x}(x,\tau)d\tau dxds = -u_0\sum_{i=1}^n E_i(t+\tau_i e^{-\frac{t}{\tau_i}}-\tau_i) \tag{22}$$

we conclude from Eqs. (20)-(22) that

$$Q(t) = -\frac{1}{L}\left(\int_0^L\int_x^L u(y,t)dydx - D^*u_0t - D_vu_0\sum_{i=1}^n E_i(t+\tau_i e^{-\frac{t}{\tau_i}}-\tau_i)\right). \tag{23}$$

Eq. (23) and the definition of t_{lag} yield the following equation

$$\int_0^L\int_x^L u^S(y)dydx = t_{lag}u_0(D-D_vE_0) - D_vu_0\sum_{i=1}^n E_i\tau_i, \tag{24}$$

where u^S stands for the steady state of u.

The Laplace transform operator is applied to Eq. (4) to determine u^S

$$\overline{u}(x,p) = \frac{u_0}{p}\frac{\sinh\delta(L-x)}{\sinh\delta L}, \tag{25}$$

where $\overline{u}(x,p)$ represents the Laplace transform of $u(x,t)$,

$\overline{u}(x,p) = \int_0^\infty e^{-pt}u(x,t)dt,$

$$\delta = \pm\sqrt{\frac{p}{D + D_v\overline{k}(p) - D_vE_0 - D_v\sum_{i=1}^n E_i}} \tag{26}$$

and

$$\overline{k}(p) = \sum_{i=1}^n E_i\frac{1}{\tau_i p+1}.$$

Application of the Final Value Theorem leads to $u^s(x) = \lim_{p\to 0} \overline{u}(x,p)$ and, consequently,

$$u^S(x) = u_0 \frac{L-x}{L}. \tag{27}$$

Replacing the expression of $u^s(x)$ in Eq. (24) gives

$$t_{lag} = \frac{\frac{L^2}{6} + D_v \sum_{i=1}^{n} E_i \tau_i}{(D - D_v E_0)}. \tag{28}$$

As $D - D_v E_0 > 0$, Eq. (28) gives a positive lag time, as expected . The Fickian contribution dominates the process and there is an effective penetration of the fluid in the polymer. After replacing $\tau_i = \frac{\mu_i}{E_i}$ in Eq. (28), it is clear that the lag time is independent of the Young's modulus of the Maxwell arms. It is an increasing function of elastic modulus E_0 of the free spring and the global viscosity $\sum_{i=1}^{n} \mu_i$.

Figure 3 shows t_{lag} as a function of E_0. A Maxwell generalized model with $n = 1$ is used. The following parameters are set:$\Omega = [0, 10^{-3}]$, $u_0 = 1$, $L = 10^{-3}$, $D = 3 \times 10^{-3}$, $D_v = 10^{-6}$, $E_1 = 10$, and $\mu = 10^{-5}$. As E_0 increases, the steady-state flux decreases and the lag time increases. The role of E_0 is to lower the effective diffusion coefficient of the fluid. The crosslink density of the matrix can be quantified by $\frac{E_0}{3RT}$, where R is the universal constant and T is the absolute temperature. As E_0 is raised, the crosslink density increases, which leads to a large degree of entanglement in the polymer. The net effect of this change is a delay in the transport of the solute.

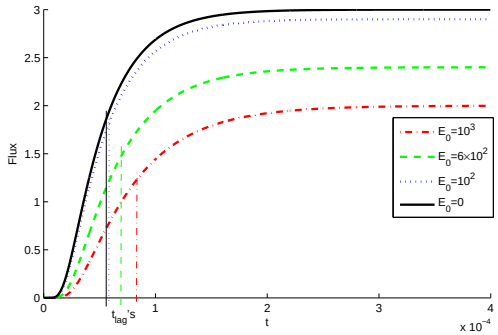

FIGURE 3. Behavior of the flux and t_{lag} for different E_0.

2.2.2. *Effective time constant.* The effective time constant indicates the time elapsed before reaching a steady-state condition. This measure has been first proposed in [2] and lately addressed in [8], [20], [21] and [22].

Following [2], t_{eff}, is calculated by

$$t_{eff} = \frac{\int_0^\infty (J(L,s) - J^S) s ds}{\int_0^\infty J(L,s) - J^S ds}, \tag{29}$$

where J^S represents the steady flux.

While the lag time monitors the first appearance of the diffusing fluid, t_{eff} measures the onset of an equilibrium state. In fact, it can be proved, using a statistical interpretation ([8], [9]), that for $t = 4t_{eff}$, we have $J(L, 4t_{eff}) = 98.17\% J^S(x)$ for a first-order system.

Equation (29) can be applied without explicit knowledge of the analytical form of the flux. As pointed out in [2], if the Laplace transform of $J(L,t)$, $\overline{J}(L,p)$, can be written as

$$\overline{J}(L,p) = \frac{1}{p}(B_1 + B_2 p + B_3 p^2) + \dots \tag{30}$$

for p small and where $B_2 \neq 0$, then $t_{eff} = -\dfrac{B_3}{B_2}$.

As

$$\overline{J}(x,p) = -(D - D_v \widehat{E}) \overline{\frac{\partial u}{\partial x}} - D_v \sum_{i=1}^{n} \frac{E_i}{1 + p\tau_i} \overline{\frac{\partial u}{\partial x}}, \tag{31}$$

we have from Eqs. (25) and (31)

$$\overline{J}(L,p) = \left(D - D_v \widehat{E} + D_v \sum_{i=1}^{n} \frac{E_i}{1 + p\tau_i} \right) u_0 \frac{\delta}{\sinh \delta L}, \tag{32}$$

where δ is defined in Eq. (26). Eq. (32) can be written in the form:

$$\overline{J}(L,p) = -\frac{u_0}{pL} \frac{1}{\frac{1}{w} + \frac{p}{w^2}\frac{L^2}{3!} + \frac{p2}{w^3}\frac{L^4}{5!} \dots}, \tag{33}$$

with

$$w(p) = D - D_v \widehat{E} + D_v \sum_{i=1}^{n} \frac{E_i}{1 + p\tau_i}. \tag{34}$$

Using the Final Value Theorem the steady-state flux becomes

$$J^S(L) = \frac{u_0}{L}(D - D_v E_0). \tag{35}$$

Therefore, $J^S(L)$ is a decreasing function of E_0 and, consequently, of the crossslink density, which is a physically sound result. Using the inequality

$$D > D_v E_0,$$

an effective release of the permeant fluid occurs.

The effective time constant is calculated from Eqs. (29)-(34):

$$t_{eff} = \frac{1}{D - D_v E_0} \frac{D_v (D - D_v E_0) \sum_{i=1}^{n} \mu_i \tau_i + \frac{7L^4}{360}}{D_v \sum_{i=1}^{n} \mu_i + \frac{L^2}{3!}}. \tag{36}$$

When the relaxation times τ_i are replaced by μ_i / E_i, it is clear that t_{eff} is a function of the Young's modulus E_i of the Maxwell arms. The effective time constant increases with τ_i.

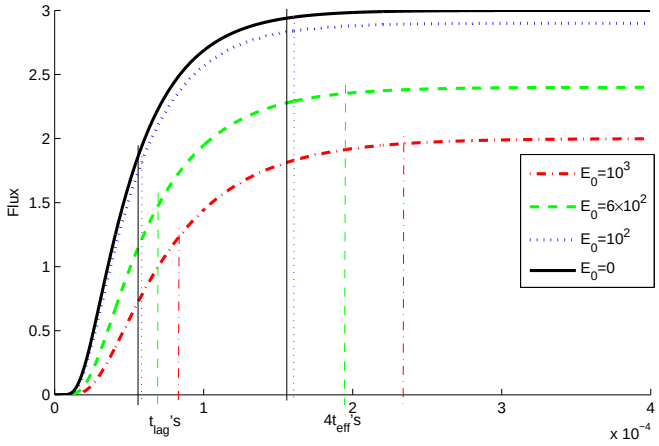

FIGURE 4. Influence of E_0 for Maxwell generalized with $n = 1$.

The influence of E_0 is illustrated in Figure 4. As E_0 increases, J^S decreases (Eq.(35)) and t_{eff} increases (Eq.(36)). The steady state flux is not very sensitive to variations in E_1 (Figure 5 - left) and in μ (Figure 5 - right). The parameters used in this simulations are the those used to generate the plot in Figure 3.

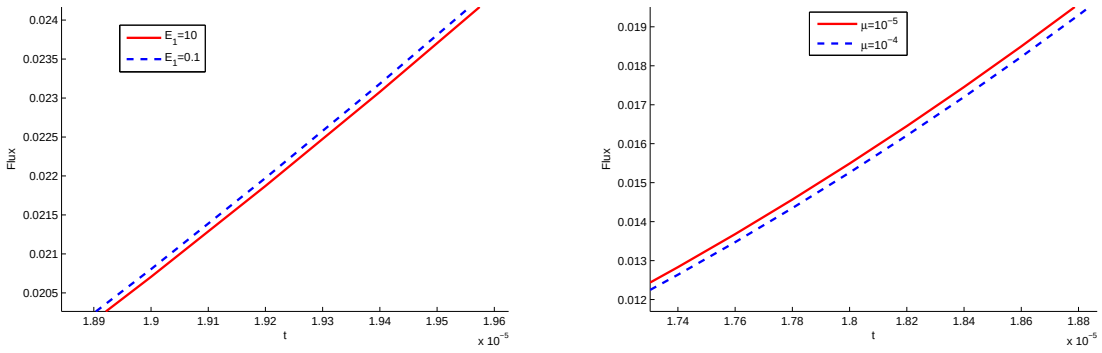

FIGURE 5. Influence of E_1 and μ for Maxwell generalized with $n = 1$.

3. A General Mechanistic-Chemical Model

3.1. Mass Flux. The transport of a fluid across the viscoelastic matrix Ω, represented in Figure 1, and in the presence of a chemical reaction is described in this section. We address the case of molecular binding which is an interaction between the fluid molecules and specific sites in the matrix. The binding is in most cases reversible. Therefore the ligand and receptor will join and divide repeatedly. While the stress function is still described by the generalized Maxwell model, the penetrant is allowed to bind reversibly to the viscoelastic matrix:

$$\begin{cases} \dfrac{\partial u}{\partial t} = \nabla.(D\nabla u) + \nabla.(D_v \nabla \sigma) + f(u,v) \text{ in } \Omega \times \mathbb{R}^+, \\ \dfrac{\partial v}{\partial t} = g(u,v) \text{ in } \Omega \times \mathbb{R}^+, \\ \sigma = -\displaystyle\int_0^t (E_{0+} \sum_{i=1}^{n} E_i e^{-\frac{t-s}{\tau_i}}) \frac{\partial \epsilon}{\partial s} ds \text{ in } \Omega \times \mathbb{R}^+, \end{cases} \tag{37}$$

where u represents the free fluid concentration, v the bound fluid concentration, D the diffusion and D_v the viscoelastic diffusion. The functions f and g stand for the affinity between the fluid and the polymer. We stipulate, as before, that the strain is proportional to the fluid concentration, that is

$\epsilon = \alpha u$. Therefore, we have from (37)

$$\begin{cases} \dfrac{\partial u}{\partial t} = -\nabla \cdot J + f(u,v) \text{ in } \Omega \times \mathbb{R}^+, \\ \\ \dfrac{\partial v}{\partial t} = g(u,v) \text{ in } \Omega \times \mathbb{R}^+, \end{cases} \tag{38}$$

where the flux J is defined in (8).

For simplicity the binding and unbinding rates can be described by a linear relationships. This representation is justified by the fact that the fluid U (with concentration u) binds to immobilized sites S, in the matrix, with constant concentration s. The reaction is shown by the equation $U + S \rightleftarrows V$, where V is the bound fluid. The binding step is best explained by a second order reaction, with rate $\lambda s u$ where s is constant. As a result this reaction rate can be given the form $\lambda_2 u$. When the bound fluid V becomes free there is only one reactant, so the reaction is first order of the form $\lambda_1 v$.

The function f is then defined as

$$f(u,v) = -\lambda_2 u + \lambda_1 v, \tag{39}$$

where λ_1 and λ_2 are the unbinding and binding rates, respectively ([19]). According to Eq. (39) an equilibrium can be achieved between bound and free molecules. As binding is reversible, the function g that appears in the second equation of (37) is such that $g(u,v) = -f(u,v)$. The variation of v, in the second equation of system (38), is only due to the balance between free and bound molecules, because bound molecules do not diffuse.

The system (38) is coupled with initial conditions

$$u(x,0) = 0,\ v(x,0) = 0,\ x \in \Omega \tag{40}$$

and boundary conditions

$$\begin{cases} u = u_0, \text{ on } \Gamma_{in} \times \mathbb{R}^+ \\ v = \dfrac{\lambda_2}{\lambda_1} u_0 (1 - e^{-\lambda_1 t}), \text{ on } \Gamma_{in} \times \mathbb{R}^+ \\ u = 0, \text{ on } \Gamma_{out} \times \mathbb{R}^+ \\ J = 0, \text{ on } \Gamma_{out} \times \mathbb{R}^+ \end{cases} . \tag{41}$$

Assuming that D and D_v are constant matrices, the following equation is obtained after using Eqs. (38)-(41):

$$\frac{\partial u}{\partial t} = \nabla\cdot(D-D_v\widehat{E})\nabla u+\int_0^t k(t-s)\nabla\cdot(D_v\nabla u(s))ds+\lambda_1\lambda_2\int_0^t e^{-\lambda_1(t-s)}u(s)ds-\lambda_2 u, \tag{42}$$

where D_v, $\widehat{E}$ are included in Eq. (5) and the kernel $k(s)$ is defined in Eq. (6). As before, the tilde in D_v is dropped to simplify the notation. Following the procedure in Section 2.1 we can establish a stability result for problem (42), under perturbations of the initial condition.

The flux J associated to Eq. (42) is defined in (8). Using the Final Value Theorem, J^S is written as

$$J^s = \frac{u_0}{L}(D - D_v E_0). \tag{43}$$

Therefore, the steady-state flux is not sensitive to the binding and unbinding rates.

As in Section 2 we assume uniform properties of the flow over any cross section of Ω (Figure 1), the problem can be formulated in one dimension.

3.2. Lag time. Let $\Omega = [0, L]$. The lag time is computed by first writing the temporal changes in u and v as

$$\begin{cases} \dfrac{\partial u}{\partial t} = -\dfrac{\partial J}{\partial x} + f(u,v) \text{ in } \Omega\times\mathbb{R}^+, \\ \dfrac{\partial v}{\partial t} = -f(u,v) \text{ in } \Omega\times\mathbb{R}^+, \end{cases} \tag{44}$$

where J is defined in (8). From (44) we have

$$\frac{\partial u}{\partial t} + \frac{\partial v}{\partial t} = -\frac{\partial J}{\partial x}.$$

Following the Frisch method, we obtain

$$\int_0^L\int_x^L \left(\frac{\partial u}{\partial t}(y,t) + \frac{\partial v}{\partial t}(y,t)\right) dydx = -LJ(L,t) + \int_0^L J(x,t)dx.$$

After changing the order of integration in the expression on the left hand side of the last equation we obtain

$$\int_0^L x[\frac{\partial u}{\partial t}(x,t) + \frac{\partial v}{\partial t}(x,t)]dx = -LJ(L,t) + \int_0^L J(x,t)dx$$

and integrating in time gives

$$\int_0^L x[u(x,t)+v(x,t)]dx = -LQ(t) + \int_0^t \int_0^L J(x,\tau)dxd\tau. \tag{45}$$

To compute the asymptote of $Q(t)$, we calculate the steady state of u and v using the Final Value Theorem. The expression of u^s is the same as in Eq. (27). From Eqs. (37) and (41) we have

$$v(x,t) = \lambda_2 \int_0^t e^{-\lambda_1(t-\tau)} u(x,\tau)d\tau.$$

The Laplace transform of v is

$$\overline{v}(x,p) = \lambda_2 \frac{1}{p+\lambda_1}\overline{u}(x,p)$$

that is

$$\overline{v}(x,p) = u_0\lambda_2 \frac{1}{p(p+\lambda_1)} \frac{\sinh \widehat{\delta}(L-x)}{\sinh \widehat{\delta}L}, \tag{46}$$

where $\widehat{\delta}$ is defined by

$$\widehat{\delta}^2 = \frac{p(p+\lambda_1+\lambda_2)}{(p+\lambda_1)w} \tag{47}$$

and w is defined in Eq. (34). The Final Value Theorem applied to Eq. (46) results in

$$v^S(x) = u_0 \frac{\lambda_2}{\lambda_1} \frac{L-x}{L}.$$

The lag time is calculated from Eqs (45), (46) and the expression of $v^s(x)$:

$$t_{lag} = \frac{(1+\frac{\lambda_2}{\lambda_1})\frac{L^2}{6} + D_v \sum_{i=1}^{n} E_i\tau_i}{(D - D_vE_0)}. \tag{48}$$

When $D_v = 0$, we obtain $t_{lag} = (1+\frac{\lambda_2}{\lambda_1})\frac{L^2}{6D}$ as referred in [19]. When no binding occurs we have $\lambda_2 = 0$ which leads to Eq. (28).

The lag time is insensitive to the reaction rates for a constant $\frac{\lambda_2}{\lambda_1}$, as observed in [19], for reactive membranes under no mechanical stress. The prediction is not accurate because $Q(t)$ depends on the binding rate λ_2 ([19]).

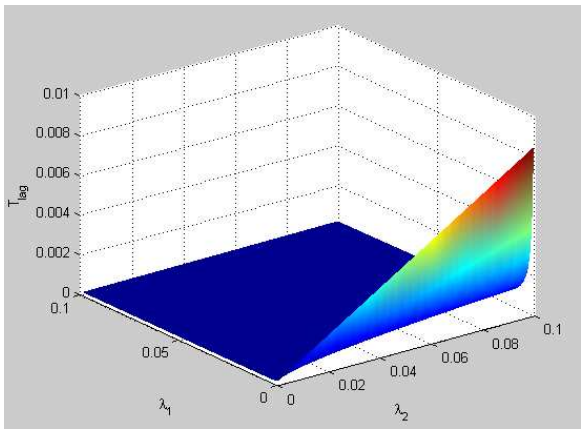

FIGURE 6. Influence of chemical reaction in t_{lag} ($\Omega = [0, 10^{-3}]$, $u_0 = 1$, $L = 10^{-3}$, $D = 3 \times 10^{-3}$, $D_v = 10^{-6}$, $E_0 = 10^3$, $E_1 = 10$).

Figure 6 shows t_{lag} as a function of λ_1 and λ_2. As expected, the lag time is an increasing function of the binding rate λ_2 and a decreasing function of the unbinding rate λ_1. These behaviors are clearly observed in Figure 6 for low values of the unbinding rate λ_1 and large values of the binding rate λ_2.

3.3. Effective time constant. The effective time constant is derived using a procedure similar to the one implemented in Section 2.2.

From Eq. (8), the Laplace transform of J is

$$\overline{J}(L,p) = \frac{u_0}{p} w(p) \frac{\widehat{\delta}}{\sinh(\widehat{\delta} L)},$$

where $w(p)$ is defined in (34) and

$$\frac{w(p)}{p} = \frac{1}{\widehat{\delta}^2} \frac{p + \lambda_1 + \lambda_2}{p + \lambda_1},$$

with $\widehat{\delta}$ given by (47).

Expanding $\sinh(\widehat{\delta} L)$ as a series, in the neighborhood of $p = 0$, $\overline{J}(L,p)$ takes the form given by Eq. (30). After some computations, t_{eff} can be written as:

$$t_{eff} = \frac{1}{D - D_v E_0} \frac{\frac{7}{360}\left(\frac{\lambda_1+\lambda_2}{\lambda_1}\right)^2 L^4 + D_v(D - D_v E_0)\sum_{i=1}^{n}\eta_i\tau_i + \left(\frac{\lambda_2}{\lambda_1^2}\right)\frac{L^2}{3!}(D - D_v E_0)}{D_v\sum_{i=1}^{n}\eta_i + \frac{L^2}{3!}\frac{\lambda_1+\lambda_2}{\lambda_1}}. \tag{49}$$

The effective time, t_{eff}, depends on λ_1 and λ_2, and not only on $\frac{\lambda_2}{\lambda_1}$ as it occurs for t_{lag}. The quantitative dependence of t_{eff} on the unbinding rate is presented in Table 1, when $\lambda_2 = 0.1$.

Figure 7 shows the effect of binding on t_{eff} when $D_v = 0$. The effective time constant decreases with an increase in the unbinding rate λ_1. For larger values of D, the influence of the unbinding rate λ_1 is less significant because diffusion becomes the driving mechanism. The time constant increases with the binding rate (Fig. 7). As D increases, the chemical effects play a minor role.

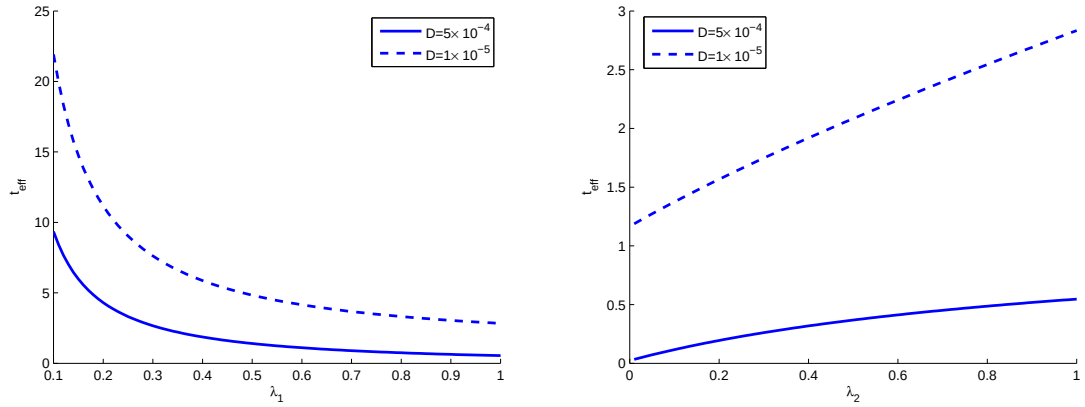

FIGURE 7. Influence of chemical reactions on t_{eff} for two diffusion coefficients, with $\lambda_2 = 1$ (left) and $\lambda_1 = 1$ (right).

In Figure 8, t_{eff} is plotted as a function of λ_1 and λ_2. When λ_2 is held constant, t_{eff} is a decreasing function of λ_1. The larger the unbinding rate, the less time it takes to reach the steady-state flux. Note that when $\lambda_2 = 0$, Eq. (36) is obtained.

Table 2 shows the effects of the reaction rates on t_{eff}. The effective time constant for the mechanistic model Section 2 is 5.833×10^{-5}. When $\frac{\lambda_2}{\lambda_1} = 1$, t_{eff} is only a function of λ_1, as shown by Eq. (49). As λ_1 increases, the equilibrium state is attained more quickly. When $\frac{\lambda_2}{\lambda_1} < 1$, the binding rate

λ_1	t_{eff}	$4t_{eff}$	$\frac{J(4t_{eff})}{J^s}$
10	0.0246	0.0984	98.236%
5	0.0277	0.1108	98.908%
1	0.1166	0.4664	99.784%
0.5	0.3613	1.4452	99.836%
0.1	5	20	99.956%

TABLE 1. Influence of λ_1 on the effective time and on the steady-state flux ($D = 5 \times 10^{-4}$, $D_v = 0$, $\lambda_2 = 0.1$, $L = 1 \times 10^{-2}$, $E_1 = 10$).

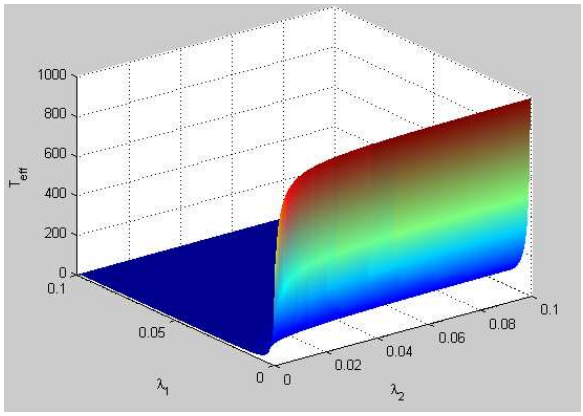

FIGURE 8. Influence of chemical reactions on t_{eff} ($\Omega = [0, 10^{-3}]$, $u_0 = 1$, $L = 10^{-3}$, $D = 3 \times 10^{-3}$, $D_v = 10^{-6}$, $E_0 = 10^3$, $E_1 = 10$).

	$\lambda_1 = \lambda_2 = 10^{-3}$	$\lambda_1 = \lambda_2 = 0.1$	$\lambda_1 = 10^{-3}$, $\lambda_2 = 0.1$	$\lambda_1 = 0.1$, $\lambda_2 = 10^{-9}$
t_{eff}	499.9851	5	990.1043	5.843×10^{-5}

TABLE 2. Effective time constant for problem (37) for different values of λ_1 and λ_2 ($\Omega = [0, 10^{-3}]$, $u_0 = 1$, $L = 10^{-3}$, $D = 3 \times 10^{-3}$, $D_v = 10^{-6}$, $E_0 = 10^3$, $E_1 = 10$).

is smaller than the unbinding rate, a condition which promotes molecular transport. Chemical affinity always induces a delay when compared with diffusion through a membrane where only mechanical effects are modelled. For a small binding rate λ_2, t_{eff} estimated from Eq. (49), approaches the value predicted by Eq. (36).

	$t_{eff}=2,\ J^s=1$	$t_{eff}=1,\ J^s=0.5$	$t_{eff}=10,\ J^s=0.5$
λ	0.25	0.5	0.05
D	2×10^{-3}	1.5×10^{-3}	1.5×10^{-3}

TABLE 3. Characterization of a membrane with a predefined flux profile ($u_0=1$, $L=10^{-3}$, $\mu=10^{-5}$, $D_v=10^{-6}$, $E_0=10^3$, $E_1=10$, $\lambda=\lambda_1=\lambda_2$).

	$t_{eff}=2,\ J^s=2\times10^{-4}$	$t_{eff}=2,\ J^s=2$	$t_{eff}=10,\ J^s=0.5$
λ	0.6	0.25	0.05
E_0	3000	1000	2500

TABLE 4. Mechanical and chemical characterization of a chemical and mechanical properties of a membrane with a predefined flux profile ($u_0=1$, $L=10^{-3}$, $\mu=10^{-5}$, $D=3\times10^{-3}$, $D_v=10^{-6}$, $E_1=10$).

Equations (43), (48) and (49) can be used to design systems with predefined steady-state fluxes. This approach leads to the estimation of the binding/unbinding rates, the diffusion coefficient or the Young modulus.

Some numerical results are shown in Tables 3 and 4. The effective time constant and steady-state flux were a priori fixed (Table 3). The parameter λ is such that $\lambda=\lambda_1=\lambda_2$. As the steady-state flux (43) in the second column is half the value of the flux in the first column, we have

$$D^{(2)}-D_vE_0=\frac{1}{2}(D^{(1)}-D_vE_0), \tag{50}$$

where $D^{(i)}$ is the value of diffusion in column (i), $i=1,2$. From Eq. (50) we obtain

$$D^{(2)}=\frac{1}{2}D^{(1)}+\frac{1}{2}D_vE_0.$$

The diffusion in the conditions of column 2 is larger than $\frac{1}{2}D^{(1)}$ because mechanical effects are present. If $D_v=0$, we have $D^{(1)}=\frac{1}{2}D^{(2)}$. As $\frac{\lambda_2}{\lambda_1}=1$, an unbinding rate larger than the one listed in column 1 must be considered to set a smaller effective time constant in column 2. The diffusion coefficients in the second and third columns are equal because the flux is the same in both cases. As λ decreases to 0.05, it takes a longer time to reach the steady-state flux (Column 3).

In Table 4, values of λ and E_0 are selected such that the predefined values for the effective time constant and steady-state flux are achieved. The Young's modulus E_0 of the free spring is chosen so that the steady-state flux satisfies Eq. (43). As E_0 decreases, t_{eff} and the stress exerted by the polymer on the penetrant decreases. Considering that in column 2 the effective time is the same as in column 1, the value of the unbinding rate must decrease. A similar trend is observed in column 3.

4. Conclusions

This paper presents a model of transport of a permeant fluid through a viscoelastic material where reversible binding can occur. The model assumes that the polymer offers a resistance to the diffusion, by exerting a stress on the incoming fluid. The physical intuition that the fickian diffusion should dominate the non fickian one, to have effective permeation, is mathematically supported by the stability of the model. It is shown how to use the mechanical and chemical properties to "taylor" the matrix in order to obtain a predefined flux profile at the outlet boundary. This is achieved through the establishment of closed form formulas for the steady flux, the time lag and the effective time. As these expressions depend on the model parameters, an inverse problem can be solved to define the properties of the matrix. Our results provide guidelines for experimentalists because the mechanical properties of polymers can be tuned by blending together different polymers or connecting molecular chains by cross-links. Similarly the chemical properties of permeation can be changed by the inclusion of binding sites in the matrix or the use of polymers with affinities for the diffusing fluid. The qualitative dependence of the time constants on the parameters is physically sound. The main contribution of this study is the quantification of such dependence, which make it possible to tailor the mechanical and chemical properties of the matrix for specific applications.

Acknowledgements

This work was partially supported by the Centro de Matemática da Universidade de Coimbra (CMUC), funded by the European Regional Development Fund through the program COMPETE and by the Portuguese Government through the FCT - Fundação para a Ciência e Tecnologia under the project PEst-C/MAT/UI0324/2013.

Appendix A. Annex

Symbol	Definition (unities)
u	concentration of the penetrant (mol/m^3)
D	diffusion coefficient (m^2/s)
D_v	stress-driven diffusion coefficient $(mol/(m.s.Pa))$
σ	stress (Pa)
E_0	Young modulus (Pa)
E_i	Young modulus of arms (Pa)
ϵ	strain
τ_i	relaxation time (s)
μ_i	viscosity $(Pa.s)$
J	flux $(mol/(m^2.s))$
λ_1	unbinding rate (s^{-1})
λ_2	binding rate (s^{-1})
L	length of the polymeric matrix (m)
J^s	steady-state flux $(mol/(m^2.s))$
t_{eff}	effective time (s)
t_{lag}	lag time (s)

References

[1] H.F. Brinson, L.C. Brinson, Polymer engineering science and viscoelasticity, An Introduction, Springer, 2008.

[2] R. Collins, The choice of an effective time constant for diffusive processes in finite systems, J. Phys. D Appl. Phys., 13, 19-37, 1980.

[3] J. Crank. The mathematics of diffusion, Oxford University Press, 2^{nd} edition, 1980.

[4] D.A. Edwards, R. Cairncross, Desorption overshoot in polymer-penetrant systems: asymptotic and computational results, SIAM J. Appl. Math., 63, 98-115, 2002.

[5] D.A. Edwards, D.S. Cohen, A mathematical model for a dissolving polymer, AIChE J., 18, 2345-2355, 1995.

[6] J.A. Ferreira, M. Grassi, E. Gudino, P. de Oliveira, A new look to non-Fickian diffusion, to appear in App. Math. Model.

[7] J.A. Ferreira, M. Grassi, E. Gudino, P. de Oliveira, A 3D model for mechanistic control drug release, SIAM J. Appl. Math., 74, 620-633, 2014.

[8] J.A. Ferreira, P. de Oliveira, P.M. da Silva, L. Simon, Flux tracking in delivery polymeric systems, Appl. Math. Model., 35, 4684-4696, 2011.

[9] J.A. Ferreira, P. de Oliveira, P. da Silva, Analytics and numerics of drug release tracking, J. Comput. Appl. Math., 236, 3572-3583, 2012.

[10] A. Friedman, Monotonicity solution of volterra integral equations in banach space, Trans. American Math. Soc., 138, 129-148, 1969.

[11] A. Friedman, M. Shinbrot, Volterra integral equations in banach space, Trans. American Math. Soc., 126, 131-179, 1967.

[12] H.L. Frisch. The Time Lag in Diffusion, J. Phys. Chem., 61, 93-95, 1957.

[13] C. F. C. M. Fong, C. Moresoli, S. Xiao, Y. Li, J. Bovenkamp, D. De Kee, Modeling diffusion through geomembranes, J. Appl. Polym. Sci., 67, 1885-1889, 1998.

[14] R. Gaspar, R. Duncan, Polymeric carriers: preclinical safety and the regulatory implications for design and development of polymer therapeutics, Adv Drug Delivery Rev., 12, 61, 1220-31, 2009.
[15] C.L. Huang, T.W.J. Steele, E. Widjaja, F.Y.C. Boey, S.S. Venkatraman, J.S.C. Loo, The influence of additives in modulating drug delivery and degradation of PLGA thin film, NPG Asia Materials, 5, 1-11,2013.
[16] M. Jelvehgari, H. Valizadeh, F. Kiafarab, L. Afandipourc , Taste masking and characterization of chlorpheniramine maleate by using enteric polymers carrier system, J. Rep. Pharm. Sci., 2, 45-58, 2013.
[17] Q. Liu, X. Wang, D. De Kee, Mass transport through swelling membranes, Int. J. Eng. Sci., 43, 1464-1470, 2005.
[18] R.A. Siegel, Characterization of relaxation to steady state in membranes with binding and reaction, J. Memb. Sci., 251, 91-99, 2005.
[19] R.A. Siegel, E.L. Cussler, Reactive barrier membranes: some theoretical observations regarding the time lag and breakthrough curves, J. Memb. Sci., 229, 33-41, 2004.
[20] L. Simon, Analysis of heat-aided membrane controlled drug released from a process control prespective, Int. J. Heat Mass Transfer, 50, 2425-2433, 2007.
[21] L. Simon, Timely drug delivery from controlled-release devices: Dynamic analysis and novel design concepts, Math. Biosci., 217, 151-158, 2009.
[22] L. Simon, Control of biological and drug-delivery systems, John Wiley and Sons,New Jersey, USA, 2013.
[23] A. Strzelewicz, Z. J. Grzywna, On the permeation time lag for different transport equations by Frisch method, J. Memb. Sci., 322, 460-465, 2008.
[24] G. Thilagavathi, A.S.M. Raja , T. Kannaian, Nanotechnology and protective clothing for defence personnel, Defence Sci. J., 58, 4, 451-459, 2008.
[25] V. Thomée, L. Wahlbin, Long-time numerical solution of a parabolic equation with memory, Math. of Coump., 62, 477-496, 1994.
[26] S. Xiao, C. Moresoll, J. Bovenkamp, D. De Kee, Sorption and permeation of organic environmental contaminants through PVC geomembranes, J. Appl. Polym. Sci., 63, 1189-1197, 1997.

J.A. Ferreira
CMUC-Department of Mathematics, University of Coimbra, Apartado 3008, 3001-454 Coimbra, Portugal

E-mail address: ferreira@mat.uc.pt
URL: http://www.mat.uc.pt/~ferreira

P. de Oliveira
CMUC-Department of Mathematics, University of Coimbra, Apartado 3008, 3001-454 Coimbra, Portugal

E-mail address: poliveir@mat.uc.pt

P.M. da Silva
Instituto Politécnico de Coimbra, ISEC, DFM, Rua Pedro Nunes, 3030-199 Coimbra, Portugal. CMUC.

E-mail address: pascals@isec.pt

Laurent Simon

Otto H. York Department of Chemical, Biological and Pharmaceutical Engineering, New Jersey Institute of Technology.

E-mail address: laurent.simon@njit.edu